Activation of liver X receptor plays a central role in antiviral actions of 25-hydroxycholesterol

Ying Liu,[1,*,†] Zhuo Wei,[1,§] Ye Zhang,[§] Xingzhe Ma,[**] Yuanli Chen,[*] Miao Yu,[§] Chuanrui Ma,[§] Xiaoju Li,[§] Youjia Cao,[§] Jian Liu,[*] Jihong Han,[*,§] Xiaoxiao Yang,[2,*] and Yajun Duan[2,*]

School of Food and Biological Engineering,* Hefei University of Technology, Hefei, China; Guizhou Medical University,[†] Guiyang, China; College of Life Sciences,[§] State Key Laboratory of Medicinal Chemical Biology, Key Laboratory of Bioactive Materials of Ministry of Education, Nankai University, Tianjin, China; and Lerner Research Institute,** Cleveland Clinic, Cleveland, OH

Abstract Production of 25-hydroxycholesterol (25HC), a potent inhibitor of viral infection, is catalyzed by cholesterol 25-hydroxylase (CH25H). We previously reported that 25HC induced CH25H expression in a liver X receptor (LXR)-dependent manner, implying that LXR can play an important role in antiviral infection. In this study, we determined that activation of LXR by 25HC or synthetic ligands [T0901317 (T317) or GW3965] inhibited infection of herpes simplex virus type 1 (HSV-1) or MLV-(VSV)-GFP in HepG2 cells or RAW 264.7 macrophages. Genetic deletion of LXRα, LXRβ, or CH25H expression in HepG2 cells by CRISPR/Cas9 method increased cell susceptibility to HSV-1 infection and attenuated the inhibition of LXR on viral infection. Lack of interferon (IFN)-γ expression also increased cell susceptibility to viral infection. However, it attenuated, but did not block, the inhibition of LXR on HSV-1 infection. In addition, expression of CH25H, but not IFN-γ, was inversely correlated to cell susceptibility to viral infection and the antiviral actions of LXR. Metabolism of 25HC into 25HC-3-sulfate (25HC3S) by cholesterol sulfotransferase-2B1b moderately reduced the antiviral actions of 25HC because 25HC3S is a weaker inhibitor of HSV-1 infection than 25HC. Furthermore, administration of T317 to BALB/c mice reduced HSV-1 growth in mouse tissues. Taken together, we demonstrate an antiviral system of 25HC with involvement of LXR activation, interaction between CH25H and IFN-γ, and 25HC metabolism.—Liu, Y., Z. Wei, Y. Zhang, X. Ma, Y. Chen, M. Yu, C. Ma, X. Li, Y. Cao, J. Liu, J. Han, X. Yang, and Y. Duan. **Activation of liver X receptor plays a central role in antiviral actions of 25-hydroxycholesterol. *J. Lipid Res*. 2018.** 59: **2287–2296.**

Supplementary key words cholesterol 25-hydroxylase • 25-hydroxycholesterol-3-sulfate • interferon γ

25-Hydroxycholesterol (25HC) is produced in cells by an enzymatic reaction catalyzed by cholesterol 25-hydroxylase (CH25H). 25HC can function as an inhibitor of viral infection and an endogenous agonist of liver X receptor (LXR), a ligand-activated transcription factor. The previous studies have demonstrated the multiple biological functions of 25HC. For instance, CH25H expression and 25HC production are involved in immunological processes (1). Stimulation of macrophage Toll-like receptors can induce CH25H expression and consequently enhance 25HC production/secretion and suppress immunoglobulin A production (2).

CH25H expression in bone marrow-derived dendritic cells and macrophages can be upregulated by interferons (IFNs) (3). This finding results in the identification of CH25H as one of the IFN-stimulated genes and 25HC as a potent inhibitor of viral infection (4, 5). In vitro, 25HC can inhibit growth of multiple viruses in cells by blocking viral entry. The inhibition of viral infection by IFNs is also related to induction of CH25H expression and 25HC production (4, 5). In vivo, CH25H-deficient mice are more susceptible to viral infection than wild-type mice (4). 25HC also functions as an amplifier of inflammatory signaling via the activator protein 1 signaling pathway (6) and mediates the negative-feedback pathway of IFN signaling on interleukin 1 family cytokine production and inflammasome activity (7).

Besides antiviral infection (4, 5, 8–11), 25HC can regulate lipid/cholesterol metabolism by interacting with sterol regulatory element-binding proteins or LXR (12). LXR plays various biological roles, particularly in lipid metabolism

This work was supported by National Natural Science Foundation of China Grants 81473204 and 81773727 (to J.H.), 81573427 and 81722046 (to Y.D.), 31770863 (to Y.C.), and 81803517 (to X.Y.); Ministry of Science and Technology of the People's Republic of China Grants 2015DFA30430 and 2017YFE0110100 (to J.H., Y.D., X.Y., and Y.C.); and the Fundamental Research Funds for the Central Universities (to Y.D., X.Y., and Y.C.).

Manuscript received 20 February 2018 and in revised form 3 September 2018.

Published, JLR Papers in Press, October 11, 2018
DOI https://doi.org/10.1194/jlr.M084558

Abbreviations: Cas9, clustered regulatory interspaced short palindromic repeat-associated protein 9; CH25H, cholesterol 25-hydroxylase; CRISPR, clustered regulatory interspaced short palindromic repeat; FACS, fluorescence-activated cell sorting; 25HC, 25-hydroxycholesterol; 25HC3S, 25-hydroxycholesterol-3-sulfate; HSV-1, herpes simplex virus type 1; IFN, interferon; LXR, liver X receptor; MOI, multiplicity of infection; PWF, peritoneal washing fluid; RXR, retinoid X receptor; SULT2B1b, sulfotransferase-2B1b; T317, T0901317.

[1]Y. Liu and Z. Wei contributed equally to this work.
[2]To whom correspondence should be addressed.
e-mail: yangxiaoxiao@hfut.edu.cn (X.Y.); yduan@hfut.edu.cn (Y.D.)

(13). Binding of a ligand to LXR results in formation of a heterodimer between LXR and retinoid X receptor (RXR), the LXR/RXR complex. The LXR/RXR complex then binds to the LXR response elements in the promoter and initiates transcription of the target genes (14). Previously, we identified several LXR response elements in the CH25H promoter, and found that both 25HC and synthetic LXR ligand [T0901317 (T317) or GW3965] induced CH25H expression in different cell types. Furthermore, treatment of mice with GW3965 increased CH25H expression in liver and peritoneal macrophages (15).

Expression of CH25H can be activated by IFNs (4). Interestingly, we have reported that LXR activation induced IFN-γ expression, particularly in macrophages (16). Administration of LXR ligand to mice inhibited xenograft- or carcinogen-induced tumor growth in an IFN-γ-dependent manner (16–18). 25HC can be further metabolized into 25HC-3-sulfate (25HC3S) in a reaction catalyzed by cholesterol sulfotransferase-2B1b (SULT2B1b) (19). Taken together, these studies suggest that LXR activation, interaction between CH25H and IFN-γ, and 25HC metabolism may form an antiviral system that can regulate 25HC production and its antiviral actions, with the central role played by LXR.

MATERIALS AND METHODS

Reagents

25HC was purchased from Sigma-Aldrich (St. Louis, MO). GW3965 and T317 were purchased from Cayman Chemical (Ann Arbor, MI). 25HC3S was purchased from Avanti Polar Lipids (Alabaster, AL). Human LXRα siRNA and LXRβ siRNA, rabbit anti-CH25H polyclonal antibody, mouse anti-α-tubulin, and GAPDH monoclonal antibodies were purchased from Santa Cruz Biotechnology (Dallas, TX). Rabbit anti-herpes simplex virus type 1 (HSV-1) protein polyclonal antibody was purchased from Dako Inc. (Agilent, Santa Clara, CA); rabbit anti-LXRα, -LXRβ, -IFN-γ, and -SULT2B1b polyclonal antibodies were purchased from Proteintech (Chicago, IL).

Cell lines and viruses

RAW 264.7 cells (a murine macrophage cell line) and HepG2 cells (a human hepatic cell line) were purchased from ATCC (Manassas, VA) and cultured in complete RPMI 1640 and DMEM medium containing 10% FBS, 50 μg/ml streptomycin, 100 units/ml penicillin, and 2 mM glutamine, respectively. Primary hepatocytes were isolated from male C57BL/6 mice and IFN-γ-deficient (IFN-$\gamma^{-/-}$) mice (C57BL/6 background) as described (20, 21). HSV-1 (F strain) and MLV-(VSV)-GFP pseudotyped viruses were kindly provided by Dr. Bing He from the University of Illinois at Chicago (Chicago, IL) and Dr. Wentao Qiao from Nankai University (Tianjin, China), respectively.

cDNA synthesis and quantitative real-time PCR

Total RNA was extracted from cells followed by cDNA synthesis as described (22). Real-time PCR was conducted using SYBR Green PCR Master Mix (Bio-Rad) and the following primers: CH25H forward, 5′-ATGTTGACCACGTGGAAGGT-3′ and CH25H reverse, 5′-TGGGAACTGTTTTCTTTGGG-3′; GAPDH forward, 5′-ACAACTTTGGCATTGTGAA-3′ and GAPDH reverse, 5′-GATGCAGGGATGATGTTCTG-3′. CH25H mRNA expression was normalized to GAPDH mRNA in the corresponding samples.

Western blot analysis

After treatment, cellular proteins were extracted. Expression of CH25H, LXRα, LXRβ, IFN-γ, SULT2B1b protein, and total HSV-1 proteins in cellular lysate was determined by Western blot as described (15). Expression of GAPDH or α-tubulin was determined as loading control.

Immunofluorescent staining

After treatment, levels of HSV-1 proteins in intact HepG2 cells were determined by immunofluorescent staining as described (23). Briefly, cells were fixed with 4% paraformaldehyde for 30 min, washed with PBS for 10 min, and permeabilized in 0.5% Triton X-100/PBS for 10 min. Cells were then blocked with 2% BSA for 2 h at room temperature. After incubation with rabbit anti-HSV-1 protein antibody overnight at 4°C, cells were incubated with FITC-conjugated secondary antibody for 2 h. Cells were then stained with DAPI solution to detect the nucleus followed by observation and photographs with a fluorescence microscope (Leica, Wetzlar, Germany).

Determination of virus growth

Cells were pretreated with LXR ligand for 24 h followed by infection with HSV-1 for 2 h. After washing with PBS, cells were cultured in fresh complete medium or medium containing LXR ligand for 16 h. Cells were then lysed, followed by determination of HSV-1 proteins in cellular lysate by Western blot. The HSV-1-infected HepG2 cells were also used to determine infecting viruses by immunofluorescent staining with anti-HSV-1 protein antibody and the protocol as described above.

The inhibition of LXR ligand on HSV-1 infection in HepG2 cells was also determined by viral plaque formation assay. HepG2 cells were pretreated with 25HC or T317 for 24 h followed by HSV-1 infection for 2 h. After removal of viruses, HepG2 cells were treated with 25HC or T317 for the indicated times. The infected HepG2 cells were harvested and the infecting viruses in HepG2 cells were released by repeated freezing and thawing. The cellular lysate was collected as the source of viruses. The collected viruses were diluted with 199v medium and then added to the monolayer of Vero cells. After viral growth for more than 24 h, Vero cells were observed under a microscope and the plaques formed were counted. The virus titers were calculated and normalized by the dilution factor.

The infecting MLV-(VSV)-GFP pseudotyped viruses in HepG2 cells were determined by two methods, image assay and fluorescence-activated cell sorting (FACS) assay, based on the fact that the viruses were labeled with GFP. In an image assay, after infection, the virus-infected cells are observed under a fluorescence microscope and the cells' images are photographed. In a FACS assay, the infected cells are applied to an FACS machine to quantify infected cells, using the negative control cells (uninfected HepG2) as the set for gating. In this study, after infection and treatment, HepG2 cells were collected and then observed under a fluorescence microscope. Images of cells with fluorescence or phase contrast were photographed. For FACS assay, cells were harvested and subjected to the FACS machine directly to quantify cells containing GFP. Based on the gate with negative control cells, the percentage of MLV-(VSV)-GFP pseudotyped virus-infected cells out of total cells was determined.

CRISPR/Cas9-mediated mutations

HepG2 cells lacking LXRα, LXRβ, CH25H, or SULT2B1 expression were established using the clustered regulatory interspaced

short palindromic repeat (CRISPR)/CRISPR-associated protein 9 (Cas9) technology, respectively (24). The guide sequence was designed based on the online CRISPR Design Tool (http://tools.genome-engineering.org), and the sequences of the guide oligos are listed in **Table 1**. After ligation, HepG2 cells were transfected with plasmid of pSpCas9 (BB)-2A-Puro vector or vector ligated with guide oligos, respectively. The selection of mutated clonal cell lines was completed using the standard protocol (24), and the knockout of target genes was confirmed by Western blot. The cells lacking LXRα, LXRβ, CH25H, or SULT2B1b expression were defined as CRISPR-LXRα, CRISPR-LXRβ, CRISPR-CH25H, or CRISPR-SULT2B1b cells, while the corresponding control cells were defined as CRISPR-Ctrl cells.

In vivo study

The protocols for in vivo study with mice were approved by the Ethics Committee of Nankai University (Tianjin, China) and conform to the *Guide for the Care and Use of Laboratory Animals* published by the National Institutes of Health. BALB/c mice (~6 weeks old) were purchased from Beijing Vital River Laboratory Animal Technology Co., Ltd. (Beijing, China) and maintained at the Animal Center of Nankai University with free access to water and food. The mice were randomly divided into three groups and received the following treatment: mice in groups 1 and 2 were fed normal chow, and the mice in group 3 were fed normal chow containing T317 (5 mg/day/kg bodyweight) for 4 days. Mice in group 1 were then intraperitoneally injected with PBS (as a mock); mice in groups 2 and 3 were intraperitoneally injected with HSV-1 (5×10^5 PFU/mouse). Mice in groups 1 and 2 continued to be fed normal chow, while the mice in group 3 were fed normal chow containing T317. Seven days after viral injection, all the mice were euthanized. Mouse peritoneal fluid was first collected by lavage with PBS (2 ml/mouse), and it was named "peritoneal washing fluid (PWF)". Liver and brain samples were then collected individually. A piece of liver or brain stem was weighed and then homogenized in PBS (0.1 g/ml). HSV-1 in PWF or homogenates of liver or brain stem were released by repeated freezing and thawing, the viral titers in mouse tissues were determined by the plaque formation assay as described above.

Data analysis

All experiments were repeated at least three times, and the representative results are presented. Data are presented as mean ± SEM and were analyzed by two-tailed unpaired Student's *t*-test or post hoc test of one-way ANOVA analysis. The difference was considered significant if $P < 0.05$.

RESULTS

LXR activation inhibits infection of HSV-1 or MLV-(VSV)-GFP in HepG2 cells

CH25H has been identified as an antiviral molecule because it catalyzes the production of 25HC, a potent antiviral small chemical. In addition, CH25H is an IFN-inducible molecule (4, 5). Interestingly, we have reported that expression of hepatic CH25H or macrophage IFN-γ can be activated by LXR (15, 16). Based on the above studies, we hypothesized that LXR activation may play an important role in antiviral infection by activating CH25H expression.

To test this, we initially infected HepG2 cells with HSV-1 and determined CH25H expression in response to viral infection. In contrast to the previous report that indicates viral infection can activate macrophage CH25H mRNA expression (5), we found that HSV-1 infection had little effect on hepatic CH25H protein expression (**Fig. 1A**). This difference may be due to the fact that macrophages are a major cell type expressing IFNs, and viral infection to macrophages can induce IFN production, which, in turn, induces CH25H mRNA expression (5). Meanwhile, HSV-1 infection had little effect on 25HC- or T317-induced CH25H expression in HepG2 cells (Fig. 1B).

Next, we determined that pretreatment of HepG2 cells with 25HC or T317 reduced cellular HSV-1 protein levels in a dose-dependent manner with the greater effect by 25HC indicating either of them inhibits HSV-1 infection (Fig. 1C). The greater inhibition by 25HC than T317 should be partially attributed to the action of exogenously added 25HC. The results of immunofluorescent staining of cellular HSV-1 proteins show that the fluorescent intensity was substantially reduced by 25HC or T317 (Fig. 1D), which directly demonstrates that LXR activation inhibits viral infection.

To further determine inhibition of HSV-1 growth by 25HC or T317, the 25HC- or T317-pretreated HepG2 cells were infected with HSV-1, and then continually exposed to 25HC or T317 for different times. The viruses collected from the above HepG2 cells were added to Vero cells for 36 h and the formed plaques were counted. The results of the virus titer assay shown in Fig. 1E confirm that 25HC and T317 inhibited viral growth in HepG2 cells dose dependently.

To determine the effect of LXR on infection of other viruses in HepG2 cells, the pretreated HepG2 cells with LXR ligand were infected with MLV-(VSV)-GFP pseudotyped viruses. Because MLV-(VSV)-GFP pseudotyped viruses are labeled with GFP, we are able to determine viral infection using either image assay or FACS assay. As shown in **Fig. 2A**, B, LXR ligands (25HC, T317, or GW3965) inhibited growth of MLV-(VSV)-GFP pseudotyped viruses in a dose-dependent manner. To determine the role of LXR or CH25H expression in antiviral infection, we selectively inhibited LXR or CH25H expression by transfecting cells with the corresponding siRNA. Indeed, inhibition of LXR or CH25H expression by siRNA increased the cells' susceptibility to MLV-(VSV)-GFP pseudotyped virus infection, while the inhibition of viral infection by T317 or 25HC was attenuated (Fig. 2C, D).

TABLE 1. Sequences of the single guide RNA for CRISPR/Cas9 system

Gene Name	20 nt Guide Sequence
LXRα (NR1H3)	TCGGCTTCGCAAATGCCGTC
LXRβ (NR1H2)	ACCCCGGCAGGCATAGCGCC
CH25H	CAGGCAAAAGCCCACGTATG
SULT2B1b	TGTCGTCGTCCCGCACATCT

The antiviral action of 25HC mainly depends on LXR-induced CH25H expression

We created HepG2 cells lacking either LXRα or LXRβ expression by CRISPR-Cas9 method (right half of **Fig. 3A**, D) and infected control HepG2 cells or LXRα or LXRβ

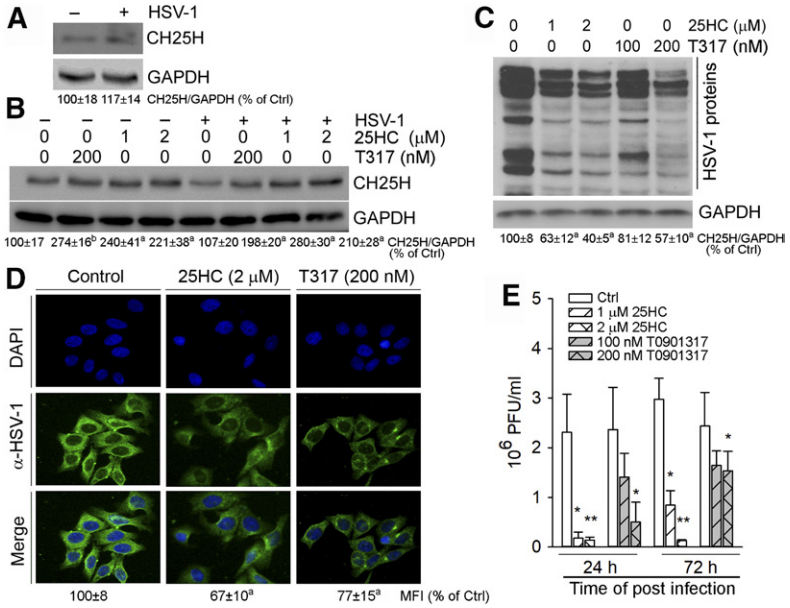

Fig. 1. 25HC and T317 inhibit HSV-1 infection in HepG2 cells. A–D: HepG2 cells or cells receiving 24 h LXR ligand pretreatment, as indicated, were infected with HSV-1 [multiplicity of infection (MOI) = 0.05] for 2 h and then switched to fresh complete medium or medium containing the same treatment for another 16 h. CH25H expression (A, B) and HSV-1 infection (C) were determined by Western blot. The bands from three repeated experiments were scanned and the density of the bands was quantified. The sum of band density from each sample was used to conduct statistical analysis. $^{a}P < 0.05$, $^{b}P < 0.01$ versus control (n = 3); HSV-1 infection was also determined by immunofluorescent staining of HSV-1 proteins in intact HepG2 cells and the mean of fluorescent intensity (MFI) from three repeated experiments was quantified and statistical analysis was conducted. $^{a}P < 0.05$ versus control (n = 3) (D). E: Inhibition of HSV-1 infection in HepG2 cells by 25HC or T317 was determined by the viral plaque formation assay. $*P < 0.05$, $**P < 0.01$ versus control (n = 3).

knockout HepG2 cells with HSV-1. Compared with CRISPR-Ctrl cells, more viral infection was determined in CRISPR-LXRα or CRISPR-LXRβ cells (Fig. 3A, D) indicating that deficiency of LXRα or LXRβ expression increased cell susceptibility to HSV-1 infection. 25HC substantially inhibited HSV-1 infection in CRISPR-Ctrl cells. However, the inhibition was clearly attenuated in cells lacking LXRα or LXRβ expression (Fig. 3B, E). The results in Fig. 3C and F demonstrate that although T317 moderately inhibited HSV-1 infection in CRISPR-Ctrl cells, it had little effect on viral infection in CRISPR-LXRα or CRISPR-LXRβ cells. The reduced inhibition or noninhibition of viral infection by 25HC or T317 was due to the induction of CH25H expression being impaired in CRISPR-LXRα or CRISPR-LXRβ cells (Fig. 3B, C, E, F) (15).

The direct evidence demonstrating the importance of LXR-induced CH25H expression in 25HC-inhibited viral infection was obtained by the following experiment. HepG2 cells lacking CH25H expression (CRISPR-CH25H cells, Fig. 3G) were cultured in fresh medium for 24 h.

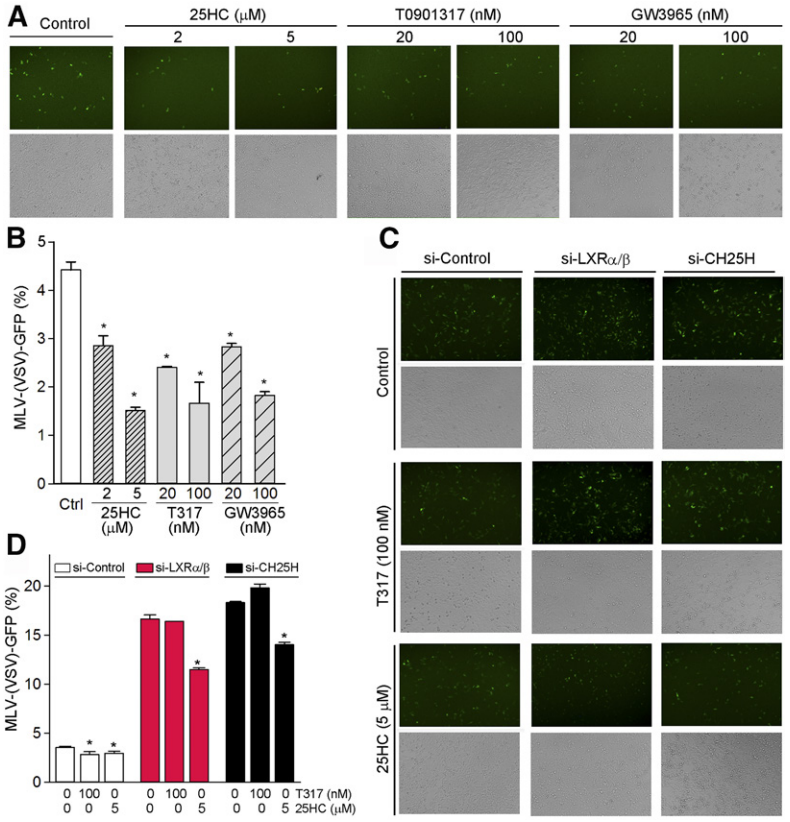

Fig. 2. T317, GW3965, and 25HC inhibit infection of MLV-(VSV)-GFP pseudotyped viruses in HepG2 cells in an LXR-dependent manner. A, B: HepG2 cells were pretreated with synthetic LXR ligand (T317 or GW3965) or 25HC at the indicated concentrations for 24 h followed by infection with MLV-(VSV)-GFP pseudotyped viruses in the absence or presence of LXR ligand for 16 h. C, D: HepG2 cells were transfected with LXRα/β or CH25H siRNA (50 nM of each) for 24 h, and then infected with MLV-(VSV)-GFP pseudotyped viruses plus T317 or 25HC treatment as indicated. The viral infection was determined by the image assay (A, C) or the FACS assay (B, D). $*P < 0.05$ versus control in the corresponding groups (n = 6).

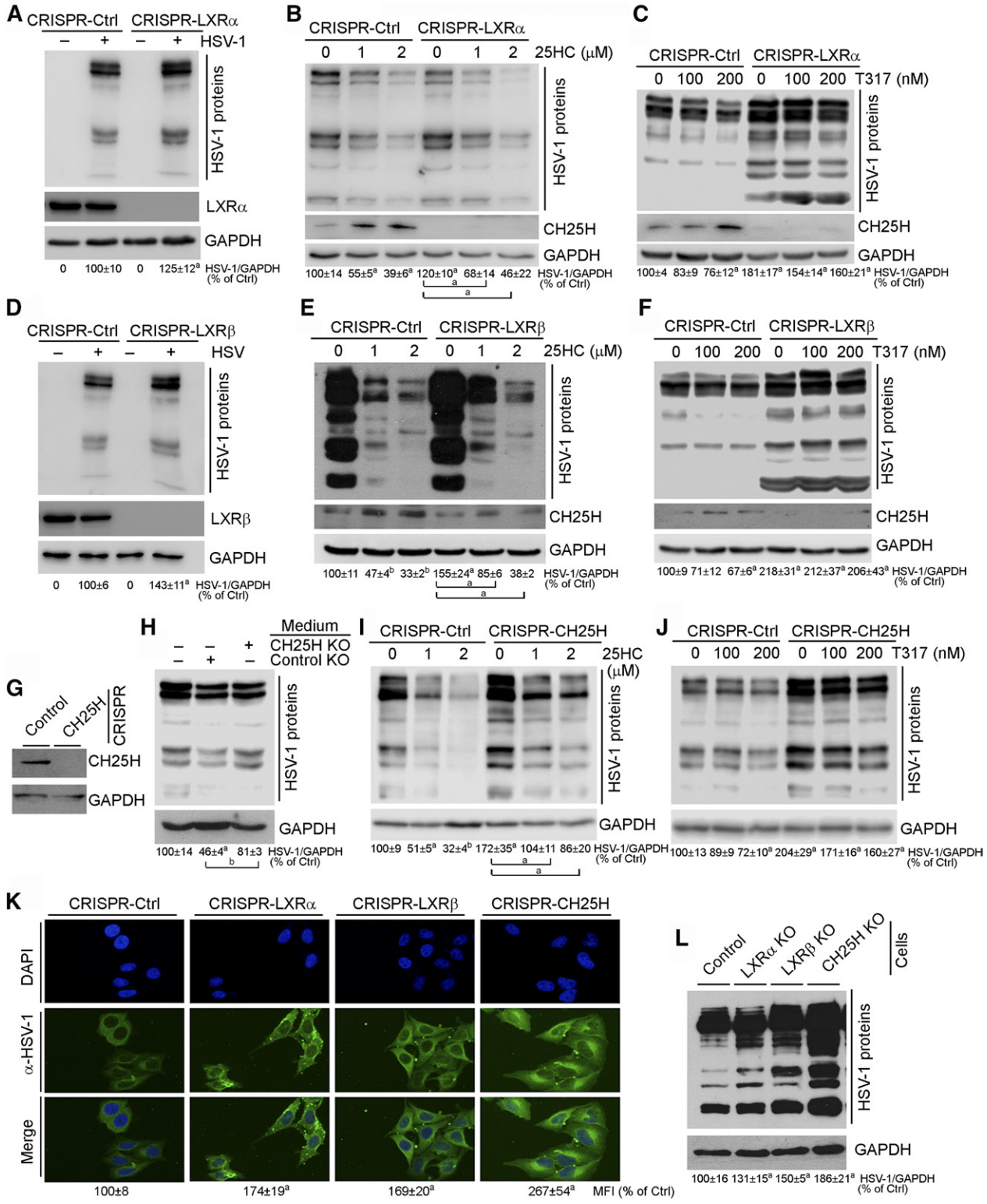

Fig. 3. Inhibition of HSV-1 infection in HepG2 cells by 25HC or T317 is determined by activation of CH25H expression in an LXR-dependent manner. A–F: CRISPR-Ctrl, CRISPR-LXRα, and CRISPR-LXRβ cells were directly (A, D) infected or infected after 16 h of T317 or 25HC pretreatment (B, C, E, F), with HSV-1 (MOI = 0.05) for 2 h. Cells were then cultured in fresh complete medium or medium containing T317 or 25HC for another 16 h. G: Deficiency of CH25H expression in CRISPR-CH25H cells was confirmed. H: HepG2 cells were infected with HSV-1 (MOI = 0.05) for 2 h and then cultured in normal complete medium or the conditioned medium collected from CRISPR-Ctrl or CRISPR-CH25H cells (24 h culture) for 16 h. I, J: CRISPR-Ctrl and CRISPR-CH25H cells received the same treatment as in B and C. K, L: CRISPR-Ctrl, CRISPR-LXRα, CRISPR-LXRβ, or CRISPR-CH25H cells were infected with HSV-1 (MOI = 0.05) for 2 h, and cells were then cultured in fresh complete medium for 16 h. Expression of CH25H protein (B, C, E–G), LXRα or LXRβ protein (A or D), and HSV-1 infection were determined by Western blot (A–F, H–J, L) or immunofluorescent staining (K). [a]$P < 0.05$, [b]$P < 0.01$ versus control or as indicated (n = 3).

The conditioned media were collected from CRISPR-Ctrl and CRISPR-CH25H cells, respectively, and then used to culture HSV-1 pre-infected HepG2 cells for 16 h. Compared with cells cultured in nonconditioned medium, reduced HSV-1 growth was determined in cells cultured in the conditioned medium collected from CRISPR-Ctrl cells. However, little reduction of HSV-1 growth was determined in the cells cultured in the conditioned medium collected from CRISPR-CH25H cells (Fig. 3H). The reduced viral growth in cells cultured in the conditioned medium collected from CRISPR-Ctrl cells should be attributed to the secreted 25HC. Similar to CRISPR-LXRα or CRISPR-LXRβ cells, inhibition of HSV-1 infection by 25HC or T317 was substantially reduced in CRISPR-CH25H cells (Fig. 3I, J).

To compare the effects of LXRα, LXRβ, and CH25H expression on cell susceptibility to HSV-1 infection, CRISPR-Ctrl, CRISPR-LXRα, CRISPR-LXRβ, or CRISPR-CH25H cells were infected with HSV-1 at the same titers for 24 h followed by determination of viral growth. Compared with CRISPR-Ctrl cells, Fig. 3K and L demonstrate that lack of LXRα, LXRβ, or CH25H expression increased cell susceptibility to HSV-1 infection in an order of $CH25H^{-/-} \geqslant LXR\beta^{-/-} \approx LXR\alpha^{-/-}$, confirming the importance of LXR and CH25H expression in antiviral infection.

Inhibition of viral infection by LXR is correlated to activation of CH25H expression in a cell type-dependent manner

IFN-γ is an LXR target (16) while it can induce CH25H expression (4). Therefore, LXR-induced CH25H expression can be further enhanced in cells expressing IFN-γ. Reciprocally, lack of IFN-γ expression reduced, but did not block, LXR-induced CH25H expression (15). Therefore, the lack of IFN-γ expression may result in increased cell susceptibility to viral infection and reduced antiviral actions of LXR.

Similar to HepG2 cells, primary hepatocytes isolated from wild-type mice can also be infected by HSV-1 (**Fig. 4A**). Compared with wild-type hepatocytes, deficiency of IFN-γ expression moderately increased cell susceptibility to HSV-1 infection (lane 5 vs. lane 1, Fig. 4B). In addition, the antiviral actions of 25HC and T317 (lanes 2–4 vs. lane 1, Fig. 4B) were reduced in IFN-$\gamma^{-/-}$ hepatocytes (lanes 6–8 vs. lanes 2–4, Fig. 4B), which should be related to the induction of CH25H expression by IFN-γ having not occurred in IFN-γ-deficient cells.

Activation of CH25H expression by IFNs is believed to be an important antiviral mechanism of IFNs in macrophages (4, 5). LXR also induces macrophage CH25H expression (15), indicating that either T317 or 25HC can inhibit HSV-1 infection in macrophages. Initially, we compared expression patterns of CH25H and IFN-γ between HepG2 cells and RAW 264.7 macrophages, which can be used to correlate the inhibitory effect of LXR on viral infection with the levels of CH25H or IFN-γ expression. **Figure 5A** (upper panel) shows that little CH25H protein was presented in macrophages, while abundant CH25H protein was expressed by HepG2 cells. In contrast, IFN-γ was mainly expressed by macrophages, but not hepatocytes. However,

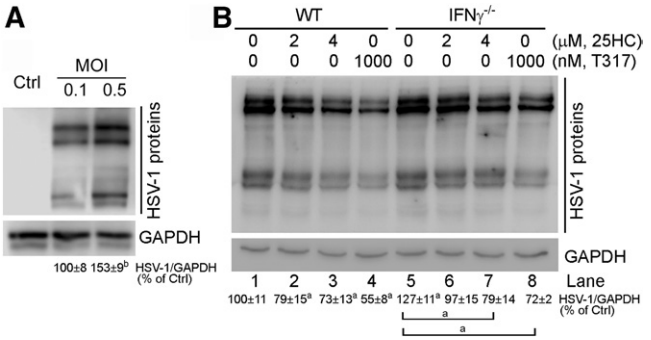

Fig. 4. Lack of IFN-γ expression reduces, but does not abolish, LXR-inhibited HSV-1 infection in mouse primary hepatocytes. A: Primary hepatocytes isolated from C57BL/6 mouse liver were infected with HSV-1 at the indicated MOI for 2 h. Cells were then cultured in fresh complete medium for 16 h. B: Primary hepatocytes isolated from C57BL/6 or IFN-$\gamma^{-/-}$ mouse liver were pretreated with T317 and 25HC for 24 h and then infected with HSV-1 (MOI = 0.5) for 2 h followed by T317 and 25HC treatment in fresh complete medium for 16 h. HSV-1 infection in primary hepatocytes was determined by Western blot. $^{a}P < 0.05$, $^{b}P < 0.01$ versus control or as indicated (n = 3).

25HC treatment induced IFN-γ expression in RAW 264.7 macrophages, not HepG2 cells (lower panel, Fig. 5A). In contrast, T317 substantially induced CH25H expression in HepG2 cells, while slightly affecting it in RAW 264.7 cells. Thus, CH25H protein levels in HepG2 cells are much higher than in RAW 264.7 macrophages, at both the basal level and induction by LXR (top row, Fig. 5B). The higher expression of CH25H in HepG2 cells should be related to the higher expression of LXRα/β in HepG2 cells (middle rows, Fig. 5B).

A previous study indicates that 25HC inhibits viral infection to mouse embryo fibroblasts in an LXR-independent pathway (5). We propose that the reason why T317 failed to inhibit viral growth in mouse embryo fibroblasts is due to a low basal level of CH25H or a poor response to LXR activation in the cells. Compared with HepG2 cells, when T317 concentration was increased up to 10 μM (⩾50-fold of that used in HepG2 cells), it clearly inhibited HSV-1 infection to RAW 264.7 macrophages (Fig. 5C).

The lower levels of CH25H in RAW 264.7 cells than in HepG2 cells suggest that macrophages might be more susceptible to viral infection, while T317 or 25HC may have reduced inhibitory effect on viral infection in macrophages. Indeed, in control cells, Fig. 5D or E demonstrates that more HSV-1 viruses were presented in RAW 264.7 cells than in HepG2 cells (lane 1 vs. lane 4). Meanwhile, T317 at low concentrations moderately inhibited HSV-1 infections in HepG2 cells (lane 2 or 3 vs. lane 1, Fig. 5D), but had no effect on viral infection in RAW 264.7 cells (lane 5 or 6 vs. lane 4). Similarly, 25HC had a more potent inhibitory effect on viral infection in HepG2 cells than in RAW 264.7 macrophages (Fig. 5E). Thus, the results in Fig. 5 suggest that the antiviral actions of LXR can be correlated to the basal levels of cellular CH25H protein and its response to LXR activation, and are unrelated to cellular IFN-γ protein.

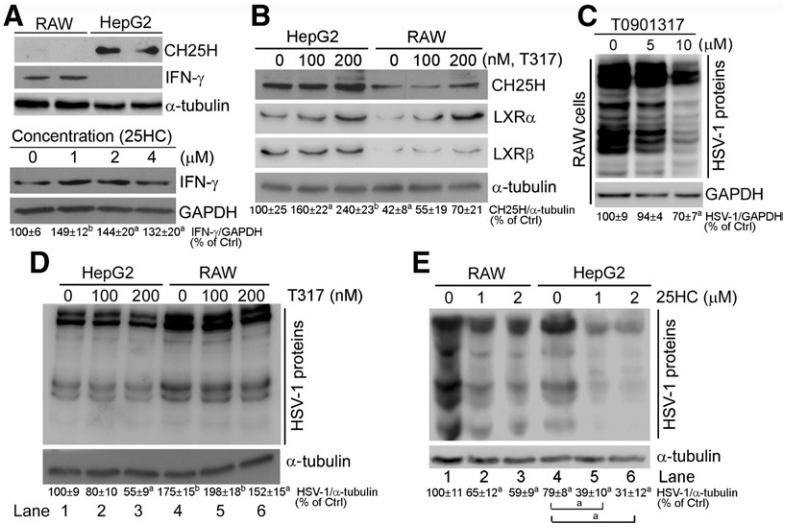

Fig. 5. Inhibition of HSV-1 infection by LXR activation is correlated to induction of CH25H expression in a cell type-dependent manner. A, B: Comparison of basal levels of CH25H and IFN-γ protein (A, upper panel) and induction of CH25H and LXR protein expression by T317 treatment for 16 h (B) between RAW 264.7 macrophages and HepG2 cells. Induction of macrophage IFN-γ expression by 25HC (A, lower panel): RAW 264.7 cells were treated with 25HC at the indicated concentrations overnight. C: RAW 264.7 macrophages were pretreated with T317 for 24 h and then infected with HSV-1 (MOI = 0.05) for 2 h and continued T317 treatment in fresh complete medium for 16 h. D, E: HepG2 and RAW 264.7 cells were treated with T317 or 25HC for 24 h and then infected with HSV-1 infection (MOI = 0.05) for 2 h and continued T317 or 25HC treatment for 16 h. Expression of CH25H, IFN-γ, LXRα, and LXRβ (A, B) and HSV-1 infection (C–E) in RAW 264.7 macrophages and HepG2 cells were determined by Western blot, respectively. $^{a}P < 0.05$, $^{b}P < 0.01$ versus control or as indicated (n = 3).

Activation of 25HC metabolism reduces its antiviral actions

SULT2B1b can convert 25HC into 25HC3S in hepatocytes (19, 25, 26), which implies that 25HC metabolism may influence its antiviral actions. Although 25HC3S can antagonize LXR activity (27–29), it induced CH25H protein and mRNA expression in a concentration-dependent manner (**Fig. 6A**, B). However, compared with 25HC, 25HC3S was a weaker activator for CH25H expression (Fig. 6C). Meanwhile, we determined that 25HC3S inhibited HSV-1 infection to HepG2 cells in a concentration-dependent manner (Fig. 6D) with a weaker effect than 25HC (lanes 2–4 vs. lanes 5–7, Fig. 6E).

The results above also indicate that SUL2B1b expression can impact the antiviral actions of 25HC by enhancing conversion of 25HC into 25HC3S. Indeed, when HepG2 cells were transfected with SULT2B1b expression vector, the high expressing SULT2B1b increased cell susceptibility to HSV-1 infection (left half, Fig. 6F). It also reduced the inhibitory effect of 25HC on HSV-1 infection (right half, Fig. 6F). In contrast, lack of SULT2B1b expression had little effect on CH25H expression, although it moderately activated LXR expression (Fig. 6G). Interestingly, deficiency of SULT2B1b expression did not reduce cell susceptibility to HSV-1 infection or influence the antiviral effects of 25HC (Fig. 6H), indicating that the endogenous SULT2B1b activity is not high enough to regulate cellular 25HC homeostasis or the antiviral actions of 25HC. Similar to CRISPR-Ctrl cells, treatment of CRISPR-CH25H cells with 25HC3S inhibited HSV-1 infection in a concentration-dependent manner (Fig. 6I), suggesting that 25HC3S inhibits viral infection directly. However, a greater inhibitory effect of 25HC3S on HSV-1 infection in CRISPR-Ctrl cells than in CRISPR-CH25H cells was determined, which should be attributed to activation of CH25H expression by 25HC3S in CRISPR-Ctrl cells (Fig. 6A, B).

T317 reduces viral growth in mouse tissues

Our results above demonstrate that LXR activation inhibits viral infection in HepG2 cells or RAW 264.7 macrophages. To determine the physiological relevance of LXR activation, we prefed BALB/c mice with normal chow or normal chow containing T317 (5 mg/day/kg bodyweight) for 4 days. Mice were then intraperitoneally injected with HSV-1 at the same titers. Meanwhile, a group of mice fed normal chow were injected with PBS as a mock treatment. After HSV-1 injection, the feeding of normal chow or normal chow containing T317 was continued for 7 days.

After HSV-1 injection, we checked food intake, water drinking, and the external appearance of the animals daily. Although we did not observe differences of food intake/water drinking among the groups with mock, HSV-1, or HSV-1 plus T317 treatment, compared with mice receiving mock treatment, mice injected with HSV-1 alone had fur with a hunched posture, piloerection, and a slight dark color. However, mice that received HSV-1 and T317 treatment had little difference of external appearance from that of mice with mock treatment (**Fig. 7A**).

The effect of T317 treatment on viral growth in vivo was determined by the plaque formation assay. At the end of the experiment, mouse peritoneal fluid was first collected by lavage with PBS followed by liver and brain samples. A piece of liver or brain stem was homogenized in PBS. HSV-1 in PWF or homogenates of liver or brain stem were released and used to determine viral titers. As shown in Fig. 7B, after injection, viral growth can occur to the liver. Treatment of mice with T317 reduced viral growth substantially in liver and peritoneal fluid, but only moderately in brain stem (Fig. 7B). Thus, the results in Fig. 7 suggest the protection of LXR against viral infection in vivo.

DISCUSSION

25HC has been well-documented as a potent antiviral molecule (4, 5, 8–11), indicating the importance of

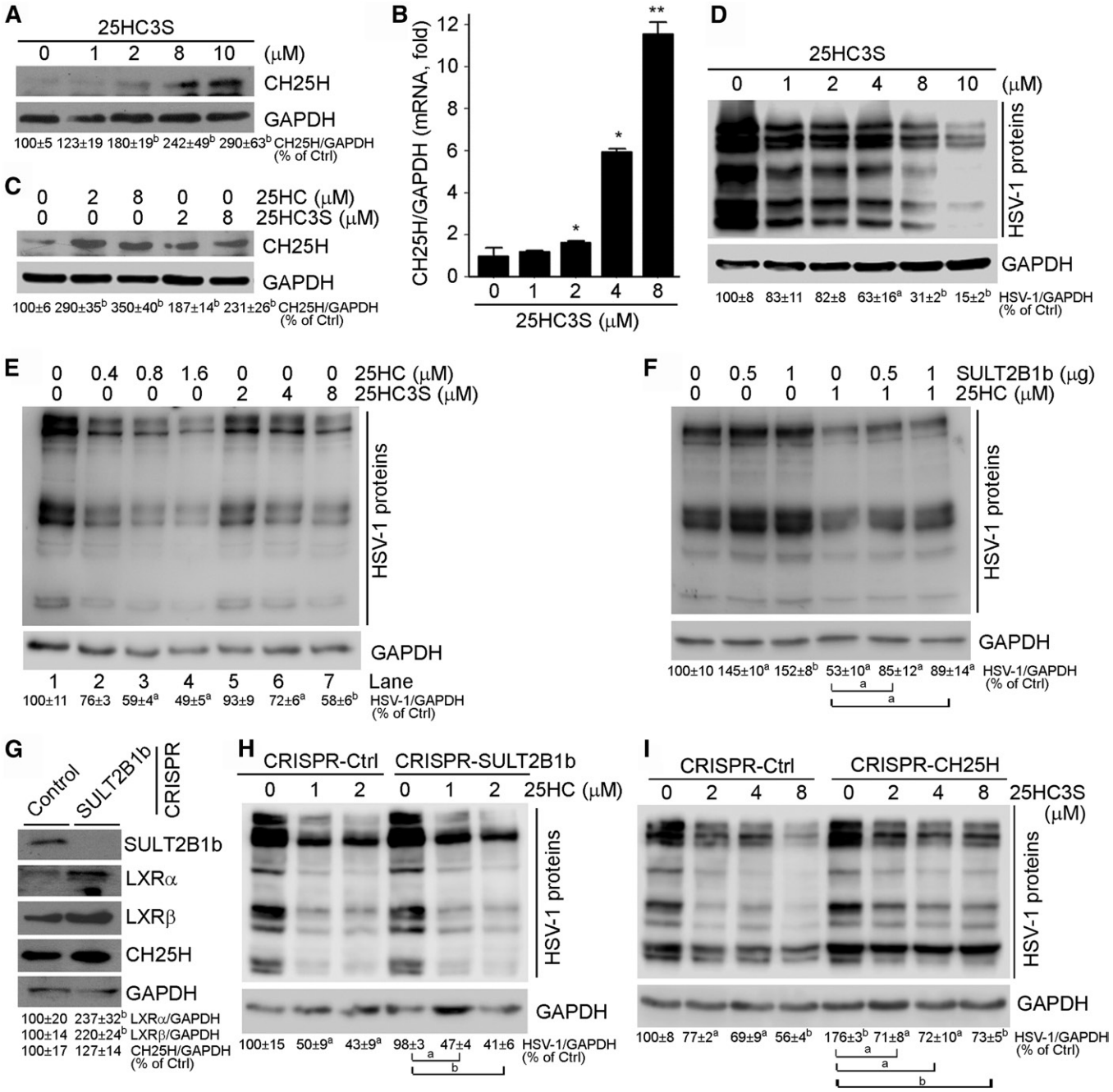

Fig. 6. 25HC3S induces CH25H expression and inhibits HSV-1 infection in HepG2 cells. A–C: HepG2 cells received the indicated treatment for 16 h (A, C) or 12 h (B). D, E: HepG2 cells were treated with 25HC3S (D), 25HC (E), or 25HC3S (E) for 24 h and then infected with HSV-1 (MOI = 0.05) for 2 h and continued treatment with 25HC3S or 25HC for 16 h. F: HepG2 cells (left half) or cells receiving 25HC pretreatment (right half, for 24 h) were transfected with SULT2B1b expression vector for 4 h and then infected with HSV-1 (MOI = 0.05) for 2 h and continued treatment with 25HC for 16 h. G: Deficiency of SULT2B1b expression in CRISPR-SULT2B1b cells was confirmed. H, I: CRISPR-Ctrl and CRISPR-SULT2B1b cells were treated with 25HC (H) or 25HC3S (I) for 24 h and then infected with HSV-1 (MOI = 0.05) for 2 h and continued treatment with 25HC (H) or 25HC3S (I) for 16 h. Expression of CH25H, SULT2B1b, LXRα, and LXRβ (A, C, G), and HSV-1 infection (D–F, H, I) were determined by Western blot. $^{a}P < 0.05$, $^{b}P < 0.01$ versus control or as indicated (n = 3). CH25H mRNA expression (B) was determined by quantitative real-time PCR. $*P < 0.05$, $**P < 0.01$ versus control (n = 6).

cellular 25HC homeostasis in antiviral actions. Cellular 25HC levels are determined by both CH25H activity and activity of the enzyme catalyzing 25HC metabolism, such as SULT2B1b (27, 30). Our previous study demonstrates that CH25H can be activated by LXR ligands, implying that LXR can inhibit viral infection (15). In the current study, we observed that T317 or GW3965 inhibited viral infection in different cell types in vitro and mouse tissues in vivo (Figs. 1, 2, 5, 7). In contrast, lack of LXR and CH25H expression increased cell susceptibility to viral infection (Figs. 2, 3), in the order of $CH25H^{-/-} \geqslant LXR\beta^{-/-} \approx LXR\alpha^{-/-}$ (Fig. 3K, L). Meanwhile, the antiviral activity of

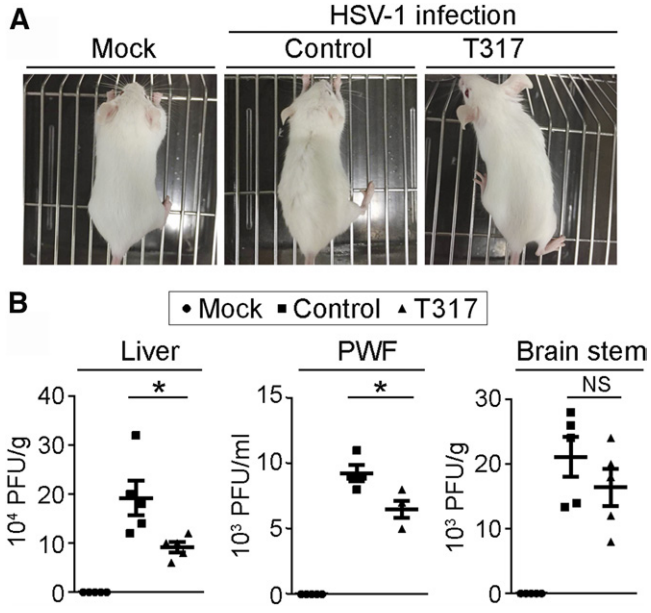

Fig. 7. Administration of T317 to mice reduces viral growth in tissues. BALB/c mice were randomly divided into three groups. Mice in the mock or control groups were fed normal chow, while mice in T317 group were fed normal chow containing T317 (5 mg/day/kg bodyweight) for 4 days. Mice in the mock group were then injected with PBS intraperitoneally and the rest mice were intraperitoneally injected with HSV-1 (5×10^5 PFU). Feeding of normal chow or normal chow plus T317 was continued for all mice. A: Mice were photographed at day 4 of viral injection. B: Seven days after viral injection, all mice were euthanized, followed by collection of PWF and liver and brain stem samples. The viral titers in mouse tissues were determined by plaque formation assay. $^*P < 0.05$ (n = 5).

LXR in these cell types was attenuated (Fig. 3C, F, J), which is attributed to either reduced induction or no induction of CH25H expression in LXRα/β$^{-/-}$ or CH25H$^{-/-}$ HepG2 cells.

CH25H is an IFN-inducible gene (3–5), while IFN-γ can be activated by LXR (16–18), indicating that IFN-γ can facilitate LXR-activated CH25H expression/25HC production and antiviral actions of 25HC. Indeed, lack of IFN-γ expression reduces basal levels of CH25H and attenuates, but does not block, LXR-activated CH25H expression (15). Consequently, lack of IFN-γ expression increased cell susceptibility to viral infection and reduced LXR-inhibited viral infection (Fig. 4). Furthermore, the expression/induction of CH25H, but not of IFN-γ, can be inversely correlated to cell susceptibility to viral infection and the antiviral effect of LXR (Fig. 5).

25HC can be metabolized into 25HC3S by SULT2B1b. Therefore, both SULT2B1b and 25HC3S may influence the antiviral actions of 25HC. Indeed, compared with 25HC, 25HC3S is a weaker activator for CH25H expression (Fig. 6C) and a weaker inhibitor of viral growth (Fig. 6E), although 25HC3S can directly inhibit viral infection (Fig. 6I). Therefore, high expression of SULT2B1b increased cell susceptibility to HSV-1 infection and attenuated 25HC-inhibited viral infection (Fig. 6F). Intriguingly, SULT2B1b expression can be activated by LXR ligands, including 25HC (31). Although LXR may induce 25HC production and IFN-γ expression in a positive loop, activation of SULT2B1b expression by LXR can enhance the conversion of 25HC into 25HC3S, which should be an important mechanism regulating 25HC/IFN-γ homeostasis to protect cells against the cytotoxicity of 25HC or IFN-γ at high concentrations.

Although 25HC/CH25H demonstrates potent antiviral functions, regulation of CH25H expression and 25HC homeostasis has not been fully understood. In this study, we found several signaling pathways that may play important roles in the antiviral actions of 25HC. Briefly, 25HC functions as an LXR ligand to induce its own production by activating CH25H expression. Meanwhile, 25HC enhances IFN-γ expression and, consequently, the activated IFN-γ feedback enhances CH25H expression/25HC production, indicating that the interaction between CH25H and IFN-γ is involved in 25HC-inhibited viral infection. Finally, SULT2B1b expression can keep 25HC-activated CH25H and IFN-γ expression under control, an important mechanism regulating 25HC homeostasis/functions. These pathways form an important antiviral infection system in which LXR plays a central role (**Fig. 8**).

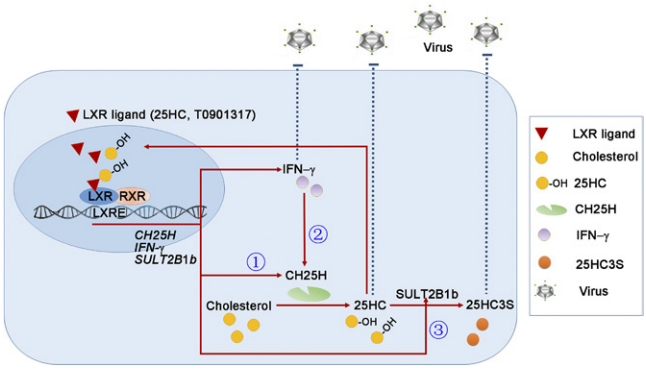

Fig. 8. The model depicts the antiviral system of LXR with involvement of activation of CH25H expression, interaction between IFN-γ and CH25H, and 25HC metabolism. Based on the results in this study and our previous report (15), we obtained the following findings: 1 (circled), 25HC functions as an LXR ligand and induces CH25H expression; 2 (circled), 25HC activates IFN-γ expression and, in turn, activated IFN-γ induces CH25H expression; 3 (circled), 25HC induces SULT2B1b expression to enhance the conversion of 25HC into 25HC3S. These three pathways work cooperatively and result in: *1*) 25HC efficiently and continuously inhibits viral infection; *2*) IFN-γ can enhance, but not determine, the antiviral actions of 25HC; and *3*) 25HC homeostasis and antiviral actions are further regulated through its metabolism by action of SULT2B1b. Furthermore, in the cells with high CH25H expression, such as hepatocytes, the auto-induction of CH25H expression/25HC production substantially increases the resistance of cells to viral infection. In contrast, in cells with low CH25H expression and high IFN-γ expression, such as macrophages, the cell susceptibility to viral infection is increased while the inhibitory effects of 25HC or LXR are reduced. Taken together, our study demonstrates an antiviral system formed by activation of CH25H expression, interaction between CH25H and IFN-γ, and 25-HC metabolism in which LXR plays a central role.

The authors appreciate that Dr. Bing He from the University of Illinois at Chicago (Chicago, IL) and Dr. Wentao Qiao from Nankai University (Tianjin, China) kindly provided HSV-1 and MLV-(VSV)-GFP pseudotyped viruses, respectively.

REFERENCES

1. Cyster, J. G., E. V. Dang, A. Reboldi, and T. Yi. 2014. 25-Hydroxycholesterols in innate and adaptive immunity. *Nat. Rev. Immunol.* **14:** 731–743.
2. Bauman, D. R., A. D. Bitmansour, J. G. McDonald, B. M. Thompson, G. Liang, and D. W. Russell. 2009. 25-Hydroxycholesterol secreted by macrophages in response to Toll-like receptor activation suppresses immunoglobulin A production. *Proc. Natl. Acad. Sci. USA.* **106:** 16764–16769.
3. Park, K., and A. L. Scott. 2010. Cholesterol 25-hydroxylase production by dendritic cells and macrophages is regulated by type I interferons. *J. Leukoc. Biol.* **88:** 1081–1087.
4. Liu, S. Y., R. Aliyari, K. Chikere, G. Li, M. D. Marsden, J. K. Smith, O. Pernet, H. Guo, R. Nusbaum, J. A. Zack, et al. 2013. Interferon-inducible cholesterol-25-hydroxylase broadly inhibits viral entry by production of 25-hydroxycholesterol. *Immunity.* **38:** 92–105.
5. Blanc, M., W. Y. Hsieh, K. A. Robertson, K. A. Kropp, T. Forster, G. Shui, P. Lacaze, S. Watterson, S. J. Griffiths, N. J. Spann, et al. 2013. The transcription factor STAT-1 couples macrophage synthesis of 25-hydroxycholesterol to the interferon antiviral response. *Immunity.* **38:** 106–118.
6. Gold, E. S., A. H. Diercks, I. Podolsky, R. L. Podyminogin, P. S. Askovich, P. M. Treuting, and A. Aderem. 2014. 25-Hydroxycholesterol acts as an amplifier of inflammatory signaling. *Proc. Natl. Acad. Sci. USA.* **111:** 10666–10671.
7. Reboldi, A., E. V. Dang, J. G. McDonald, G. Liang, D. W. Russell, and J. G. Cyster. 2014. Inflammation. 25-Hydroxycholesterol suppresses interleukin-1-driven inflammation downstream of type I interferon. *Science.* **345:** 679–684.
8. Anggakusuma, I. Romero-Brey, C. Berger, C. C. Colpitts, T. Boldanova, M. Engelmann, D. Todt, P. M. Perin, P. Behrendt, F. W. Vondran, et al. 2015. Interferon-inducible cholesterol-25-hydroxylase restricts hepatitis C virus replication through blockage of membranous web formation. *Hepatology.* **62:** 702–714.
9. Chen, Y., S. Wang, Z. Yi, H. Tian, R. Aliyari, Y. Li, G. Chen, P. Liu, J. Zhong, X. Chen, et al. 2014. Interferon-inducible cholesterol-25-hydroxylase inhibits hepatitis C virus replication via distinct mechanisms. *Sci. Rep.* **4:** 7242.
10. Xiang, Y., J. J. Tang, W. Tao, X. Cao, B. L. Song, and J. Zhong. 2015. Identification of cholesterol 25-hydroxylase as a novel host restriction factor and a part of the primary innate immune responses against hepatitis C virus infection. *J. Virol.* **89:** 6805–6816.
11. Li, C., Y. Q. Deng, S. Wang, F. Ma, R. Aliyari, X. Y. Huang, N. N. Zhang, M. Watanabe, H. L. Dong, P. Liu, et al. 2017. 25-Hydroxycholesterol protects host against Zika virus infection and its associated microcephaly in a mouse model. *Immunity.* **46:** 446–456.
12. Hong, C., and P. Tontonoz. 2014. Liver X receptors in lipid metabolism: opportunities for drug discovery. *Nat. Rev. Drug Discov.* **13:** 433–444.
13. Calkin, A. C., and P. Tontonoz. 2012. Transcriptional integration of metabolism by the nuclear sterol-activated receptors LXR and FXR. *Nat. Rev. Mol. Cell Biol.* **13:** 213–224.
14. Repa, J. J., and D. J. Mangelsdorf. 2000. The role of orphan nuclear receptors in the regulation of cholesterol homeostasis. *Annu. Rev. Cell Dev. Biol.* **16:** 459–481.
15. Liu, Y., Z. Wei, X. Ma, X. Yang, Y. Chen, L. Sun, C. Ma, Q. R. Miao, D. P. Hajjar, J. Han, et al. 2018. 25-Hydroxycholesterol activates the expression of cholesterol 25-hydroxylase in an LXR-dependent mechanism. *J. Lipid Res.* **59:** 439–451.
16. Wang, Q., X. Ma, Y. Chen, L. Zhang, M. Jiang, X. Li, R. Xiang, R. Miao, D. P. Hajjar, Y. Duan, et al. 2014. Identification of interferon-gamma as a new molecular target of liver X receptor. *Biochem. J.* **459:** 345–354.
17. Wang, Q., L. Sun, X. Yang, X. Ma, Q. Li, Y. Chen, Y. Liu, D. Zhang, X. Li, R. Xiang, et al. 2016. Activation of liver X receptor inhibits the development of pulmonary carcinomas induced by 3-methylcholanthrene and butylated hydroxytoluene in BALB/c mice. *Sci. Rep.* **6:** 27295.
18. Ma, X., Q. Wang, Y. Liu, Y. Chen, L. Zhang, M. Jiang, X. Li, R. Xiang, R. Q. Miao, Y. Duan, et al. 2015. Inhibition of tumor growth by U0126 is associated with induction of interferon-gamma production. *Int. J. Cancer.* **136:** 771–783.
19. Li, X., W. M. Pandak, S. K. Erickson, Y. Ma, L. Yin, P. Hylemon, and S. Ren. 2007. Biosynthesis of the regulatory oxysterol, 5-cholesten-3beta,25-diol 3-sulfate, in hepatocytes. *J. Lipid Res.* **48:** 2587–2596.
20. Zhou, X., Z. Yin, X. Guo, D. P. Hajjar, and J. Han. 2010. Inhibition of ERK1/2 and activation of liver X receptor synergistically induce macrophage ABCA1 expression and cholesterol efflux. *J. Biol. Chem.* **285:** 6316–6326.
21. Yao, L., C. Wang, X. Zhang, L. Peng, W. Liu, X. Zhang, Y. Liu, J. He, C. Jiang, D. Ai, et al. 2016. Hyperhomocysteinemia activates the aryl hydrocarbon receptor/CD36 pathway to promote hepatic steatosis in mice. *Hepatology.* **64:** 92–105.
22. Ma, X., Y. Liu, Q. Wang, Y. Chen, M. Liu, X. Li, R. Xiang, Y. Wei, Y. Duan, and J. Han. 2015. Tamoxifen induces the development of hernia in mice by activating MMP-2 and MMP-13 expression. *Biochim. Biophys. Acta.* **1852:** 1038–1048.
23. Zhang, L., Y. Chen, X. Yang, J. Yang, X. Cao, X. Li, L. Li, Q. R. Miao, D. P. Hajjar, Y. Duan, et al. 2016. MEK1/2 inhibitors activate macrophage ABCG1 expression and reverse cholesterol transport-an anti-atherogenic function of ERK1/2 inhibition. *Biochim. Biophys. Acta.* **1861:** 1180–1191.
24. Ran, F. A., P. D. Hsu, J. Wright, V. Agarwala, D. A. Scott, and F. Zhang. 2013. Genome engineering using the CRISPR-Cas9 system. *Nat. Protoc.* **8:** 2281–2308.
25. Ren, S., and Y. Ning. 2014. Sulfation of 25-hydroxycholesterol regulates lipid metabolism, inflammatory responses, and cell proliferation. *Am. J. Physiol. Endocrinol. Metab.* **306:** E123–E130.
26. Ren, S., P. Hylemon, Z. P. Zhang, D. Rodriguez-Agudo, D. Marques, X. Li, H. Zhou, G. Gil, and W. M. Pandak. 2006. Identification of a novel sulfonated oxysterol, 5-cholesten-3beta,25-diol 3-sulfonate, in hepatocyte nuclei and mitochondria. *J. Lipid Res.* **47:** 1081–1090.
27. Chen, W., G. Chen, D. L. Head, D. J. Mangelsdorf, and D. W. Russell. 2007. Enzymatic reduction of oxysterols impairs LXR signaling in cultured cells and the livers of mice. *Cell Metab.* **5:** 73–79.
28. Ma, Y., L. Xu, D. Rodriguez-Agudo, X. Li, D. M. Heuman, P. B. Hylemon, W. M. Pandak, and S. Ren. 2008. 25-Hydroxycholesterol-3-sulfate regulates macrophage lipid metabolism via the LXR/SREBP-1 signaling pathway. *Am. J. Physiol. Endocrinol. Metab.* **295:** E1369–E1379.
29. Bai, Q., L. Xu, G. Kakiyama, M. A. Runge-Morris, P. B. Hylemon, L. Yin, W. M. Pandak, and S. Ren. 2011. Sulfation of 25-hydroxycholesterol by SULT2B1b decreases cellular lipids via the LXR/SREBP-1c signaling pathway in human aortic endothelial cells. *Atherosclerosis.* **214:** 350–356.
30. Lund, E. G., T. A. Kerr, J. Sakai, W. P. Li, and D. W. Russell. 1998. cDNA cloning of mouse and human cholesterol 25-hydroxylases, polytopic membrane proteins that synthesize a potent oxysterol regulator of lipid metabolism. *J. Biol. Chem.* **273:** 34316–34327.
31. Jiang, Y. J., P. Kim, P. M. Elias, and K. R. Feingold. 2005. LXR and PPAR activators stimulate cholesterol sulfotransferase type 2 isoform 1b in human keratinocytes. *J. Lipid Res.* **46:** 2657–2666.